

EUR 253

VORTEX-SHEDDING FORCES AND THE FATIGUE ANALYSIS OF OFFSHORE STRUCTURES



**EUROPEAN
OFFSHORE
PETROLEUM
CONFERENCE
& EXHIBITION**

by S. Walker and S.G. Brazier, Structural Dynamics Ltd.

© Copyright 1980, European Offshore Petroleum Conference and Exhibition

This paper was presented at the European Offshore Petroleum Conference and Exhibition held in London, England, October 21-24, 1980. The material is subject to correction by the author. Permission to copy is restricted to an abstract of not more than 300 words.

ABSTRACT

This paper describes a method of incorporating vortex-shedding effects into a finite element model of a steel jacket. Recent experimental evidence has indicated fatigue rates are greater than predicted by conventional fatigue studies only incorporating direct wave loading.

The forces due to vortex shedding have been considered with reference to a large steel structure in 300 feet of water in the North Sea. These vortex shedding forces have been found to be important because they are generated with frequencies much higher than the frequency of the wave producing them. This produces effective forcing at frequencies where the dynamic natural response of the structure is appreciable.

INTRODUCTION

Recent experimental evidence indicates that the conventional fatigue analysis, which takes into account only the direct wave forcing (drag and inertia forces) is seriously underestimating the fatigue rates in offshore steel structures. This may be due to a number of factors.

- (i) The S-N curves used to estimate the number of stress cycles to failure at certain stress amplitudes are based on measurements conducted on samples in air. There are indications that sea water and the presence of cathodic protection systems can accelerate the rate of crack propagation by up to three times [1].
- (ii) Wave slam forces on horizontal, or nearly horizontal members sited near the free surface are neglected.
- (iii) Vortex shedding by members and the consequent lift forces on the structure are neglected.

References and illustrations at end of paper.

Both the effects mentioned in (ii) and (iii) give rise to forcing and consequent structural vibrations at frequencies well above the frequency associated with the waves producing them. As a result, dynamic magnification within the structure will be important.

There are a number of references dealing with the subject of wave slam [2-4]; in this paper we shall concentrate on vortex-shedding effects and their contribution to the fatigue damage of offshore steel jackets.

In the estimation of lift forces the basic experimental results and theory presented in [5] and [6] is used. The authors' contribution consists in extending the theory to the consideration of complex steel lattice structures such as the one in Figure 1. Such structures consist of many members with differing orientations each of which may exist in a different flow regime as a result of the attenuation of water-particle velocities with depth.

In addition the random phase associated with the vortex-shedding process, necessitates a statistical approach when considering neighbouring members and their interaction this is the approach set out in this paper.

As well as vortex-shedding forces direct wave, current and wind forces are included in the analysis [5] and 'Kuang' stress concentration factors [6] used for estimation of 'Hot Spots' stress levels. Miner's rule is used to calculate cumulative damage and hence estimate the fatigue life of these structures.

VORTEX SHEDDING

There are two main mechanisms of generation of vortex shedding relevant to this study

- a. Generation by steady flow
- b. Generation by oscillatory flow

When we have steady flow of a fluid past a member, vortex shedding will occur as the Reynold's number

increases to the value at which the flow becomes critical, in the sense that vortices will be shed.

Such vortex shedding occurs when the boundary layer on the obstruction separates from the surface giving rise to reversed flow downstream of the separation point. As a result, a vortex, or pair of vortices, is formed. At low Reynolds number the vortices so formed remain behind the obstruction. As the flow velocity increases the vortices may detach themselves from the member, usually from alternate sides at a definite frequency. As a vortex detaches itself it leaves behind an equal and opposite circulation of fluid around the obstacle, similar to the starting vortex around an aircraft wing. As a result the obstacle experiences a lift force in a direction perpendicular to the flow. Usually such vortices are shed from alternate sides of the member at a frequency determined, in steady flow, by the Strouhal number, defined by:

$$S = Df/V_c \dots\dots\dots(1)$$

Where D is a typical dimension of the member, V_c is the current flow velocity, f_v is the frequency of vortex shedding.

As the Reynold's number increases through 3×10^5 the Strouhal number rises sharply from 0.2 to 0.4 until at a Reynold's number of about 2×10^6 the Strouhal number drops again to 0.3. It is suggested by Lloyds that for the roughened cylinders vortex shedding will occur throughout the range of Reynold's numbers from 4×10^4 upwards.

If we suspect that vortex shedding may occur, as a first approximation we may postulate that the force per length component due to lift, F_L would be of the following form:

$$F_L(t) = C_L V_c^2 \exp(i\omega_v t) \dots\dots\dots(2)$$

Where:

V_c is the fluid velocity due to the current
 ω_v is the vortex shedding frequency, given by
 C_L is an empirical coefficient dependent on the shape, and can be written:

$$C_L = \frac{1}{2} \rho D C_d \dots\dots\dots(3)$$

Where C_d is a dimensionless number, and D is the member diameter.

F_L is perpendicular to the direction of flow and the member axis. The coefficient C_d may be taken to be 0.7 for most calculations at low Reynold's numbers [5], but it drops sharply around $Re = 5 \times 10^5$ to about 0.1. For a rough cylinder, however, it may start to increase with Re as vortex shedding is triggered by the oscillation.

In oscillatory flow around slender members we may expect vortex shedding to occur during the wave motion. The situation, however, is more complex than the one considered above for currents, because the flow is accelerating and reverses direction regularly. In many cases the flow does

not persist long enough in one direction for a 'vortex street' or wake to develop before flow reversal. The disturbance of the fluid developed in one half-cycle, of the wave will be swept back on to the member in the following half-cycle, superimposed on the approach flow. For vortex shedding to occur we would expect (from consideration of the acceleration from rest of circular cylinder) that the orbital velocity of the water particles should stay sensibly constant for three to four times the vortex shedding period. Hence dynamic lift forces are only likely to occur for long waves and small cylinders.

In the present context we are considering an accelerating flow, and a more appropriate measure of the flow regime is the Keulagan-Carpenter number

$$N_{KC} = V_m T/D \dots\dots\dots(4)$$

Where V_m is the maximum water particle velocity and T is the time period of the wave.

Keulagan and Carpenter [10] proposed that when $N_{KC} > 15$ lift forces occur; Lloyds, however, recommend that lift forces be considered for $N_{KC} > 3$. In such oscillatory flow we write

$$F_L(t) = C_L V_m^2 \exp(i\omega_v t + i\phi) \dots\dots\dots(5)$$

Where ϕ is a random phase angle, uniformly distributed in the range $[0, 2\pi]$.

The simple fatigue analysis described above cannot be used when lift forces are considered for two reasons:

- (i) the phase angle of the lift forces relative to the incident wave is indeterminate.
- (ii) the frequency of the lift force is not the same as that of the incident wave.

These difficulties are illustrated in Figure 4 which shows the one-many mapping in the transfer from wave elevation to lift forces and the consequent problems associated with evaluation nodal forces.

In order to demonstrate how these difficulties are resolved, it is necessary to consider the equations of motion involved:

$$M' \ddot{u}_L + C'_s \dot{u}_L + K' u_L = F'_L \dots\dots\dots(6)$$

Where:

C'_s is the structural damping matrix
 K' is the stiffness matrix
 F'_L is the lift-force vector
 u_L is the displacement due to lift forces.

F'_L is given by:

$$F'_L = C'_L (v' - \dot{u}_L) |v' - \dot{u}_L| e^{i\phi} \dots\dots\dots(7)$$

Here v' is a vector with magnitude varying as v is $\omega_v t$, where v_m is the maximum water particle ^m

velocity, and direction perpendicular to both the instantaneous flow and member axis. C is a 'lift matrix' constructed element by element analogous to the hydrodynamic damping matrix used in direct wave loading analysis.

Since $|v'| \gg |\dot{u}_L|$ and $\text{dir}(v' - \dot{u}_L) \approx \text{dir}(v')$ (7) may be linearised to give:

$$\underline{F}_L = \underline{C}_L v_m (v' - \dot{u}_L) \dots (8)$$

Considering the lift force on a horizontal member for simplicity, its direction rotates with frequency ω_0 , the frequency of the incident wave. The magnitude of this vector, however, varies with the vortex shedding frequency ω_v , which is assumed to be an integer multiple of ω_0 . Such a vector may be represented in complex number notation by

$$\begin{aligned} \underline{F}_L &= \underline{\tilde{F}}_L \cos(\omega_v t) \exp(i\omega_0 t) \\ &= \frac{1}{2} \underline{\tilde{F}}_L \left[\exp\{i(\omega_0 - \omega_v)t\} + \exp\{i(\omega_0 + \omega_v)t\} \right] \dots (9) \end{aligned}$$

The lift displacement vector \underline{u}_L may be decomposed into two components corresponding to the two frequencies $(\omega_0 - \omega_v)$ and $(\omega_0 + \omega_v)$. Thus:

$$\left[-(\omega_0 + \omega_v)^2 \underline{M}' + i(\omega_0 + \omega_v) \underline{C}' + \underline{K} \right] \underline{u}_L^+ = \frac{1}{2} \underline{\tilde{F}}_L \dots (10)$$

$$\left[-(\omega_0 - \omega_v)^2 \underline{M}' + i(\omega_0 - \omega_v) \underline{C}' + \underline{K} \right] \underline{u}_L^- = \frac{1}{2} \underline{\tilde{F}}_L \dots (11)$$

Where

$$\underline{u}_L^+ + \underline{u}_L^- = \underline{u}_L \dots (12)$$

(10) can therefore be written:

$$\left[-(\omega_0 + \omega_v)^2 \underline{M}' + i(\omega_0 + \omega_v) (\underline{C}'_S + \underline{V}'_m \underline{C}'_L) + \underline{K} \right] \underline{u}_L^+ = \underline{C}'_L v_m v' e^{i\phi} \dots (13)$$

For brevity, we write:

$$\omega = \omega_0 + \omega_v \dots (14)$$

$$\underline{F} = \underline{C}'_L v_m v' e^{i\phi} \dots (15)$$

$$\underline{u} = \underline{u}_L^+ \dots (16)$$

In component form, (13) may be written:

$$\underline{u}_i(\omega) = \sum_j A_{ij} F_j(\omega) \dots (17)$$

Where $\{A_{ij}\} = \{-\omega^2 M'_{ij} + i\omega (C'_{Sji} + \underline{V}'_m C'_{Lji}) + K_{ij}\}^{-1}$ (18)

Denoting the complex conjugate of a quantity by * and the expected value by $E(\cdot)$, then:

$$\begin{aligned} \sigma^2(u_i(\omega)) &= E(|u_i(\omega)|^2) = \sum_{jk} A_{ij}(\omega) A_{ik}^*(\omega) E(F_j(\omega) F_k^*(\omega)) \dots (19) \end{aligned}$$

Consider now the nature of the product $F_j(\omega) F_k^*(\omega)$. Figure 5 represents part of a structure, each element of which is acted on by a lift

force determined by the method described above. The frequencies at which these forces act is indicated by the argument. If the force on the member ij is written $2F_{ij}(\omega)$ and the force at node i (of frequency ω) is written $F_i(\omega)$, for the situation in the figure

$$F_k(\omega) = F_{jk}(\omega) + F_{kn}(\omega) \dots (20)$$

$$F_j^*(\omega) = F_{ij}^*(\omega) + F_{jk}^*(\omega) \dots (21)$$

Hence for each component:-

$$\begin{aligned} F_j(\omega) F_k^*(\omega) &= F_{jk}(\omega) F_{ij}^*(\omega) + F_{kn}(\omega) F_{ij}^*(\omega) + \\ &F_{jk}(\omega) F_{jk}^*(\omega) + F_{kn}(\omega) F_{jk}^*(\omega) \dots (22) \end{aligned}$$

Taking the expectation of both sides and remembering that the expected value of two uncorrelated variables is zero then:

$$E(F_j(\omega) F_k^*(\omega)) = E(F_{jk}(\omega) F_{jk}^*(\omega)) \dots (23)$$

and

$$\begin{aligned} E(F_k(\omega) F_k^*(\omega)) &= E(F_{jk}(\omega) F_{jk}^*(\omega)) + \\ &E(F_{kn}(\omega) F_{kn}^*(\omega)) \dots (24) \end{aligned}$$

Therefore the only non-zero terms of (19) will involve standard deviations of member forces between two nodes and diagonal terms composed of the sum of forces on the members leading into the node under consideration at the frequency considered, or

$$\begin{aligned} \sigma_{u_i}^2(\omega) &= E(|u_i(\omega)|^2) = \sum_{jk} A_{ij}(\omega) A_{ik}^*(\omega) \times \\ &(|F_k(\omega)|^2 \delta_{jk} + (\text{terms due to both ends of a particular member})) \dots (25) \end{aligned}$$

As we are working on linear assumptions we may write:

$$\underline{f} = \underline{H} \underline{u} : \underline{u} = \underline{H}^{-1} \underline{f} \dots (26)$$

Where \underline{f} are the internal element forces due to the (prescribed) displacements \underline{u} .

$\{H_{ij}\}$ is a matrix linking the internal force in element i due to a displacement at node j . The matrix is defined within the finite element system for each frequency ω .

Hence

$$\begin{aligned} \sigma_{f_i}^2 &= E(|f_i(\omega)|^2) = \sum_{kjl} H_{ij}^* A_{jk} H_{il} A_{lm}^* \\ &E(F_k(\omega) F_l^*(\omega)) \dots (27) \end{aligned}$$

Hence standard deviations of the stress variation in each element for each frequency can be obtained, and assuming a Rayleigh distribution for these stresses. We can determine the distribution of stress amplitudes at each node and frequency.

In order to calculate the cumulative damage we need to know the number of cycles to failure N at each stress range S . This is obtained from the $S-N$, 'Q' curve in [11] as

$$\log_{10} S = 2.571 - 0.242 (\log_{10} N - 4) \dots (28)$$

Hence:

$$N = N(S) = S^{-4.132} \times 10^{14.624} \dots (29)$$

where S is the stress amplitude (half stress range).

If we are considering a sea state A with probability of occurrence $P(A)$ the stress distribution at frequency ω is

$$\text{prob} (S < S < S + \delta S) = \frac{S}{\sigma^2} \exp(-S^2/2\sigma^2) \delta S = P(S) \delta S \dots (30)$$

We also need the number of seconds per year at sea state $A = T(A)$.

Therefore number of cycles in stress range $[S, S + \delta S] =$

$$\frac{\omega}{2\pi} \cdot T(A) \cdot \frac{S}{\sigma^2} \exp(-S^2/2\sigma^2) \delta S = n(S) \dots (31)$$

Therefore proportion of life consumed per year in sea state A at frequency is

$$\frac{\omega T(A) S \exp(-S^2/2\sigma^2) \delta S}{2\pi \sigma^2 N(S)} \dots (32)$$

Therefore proportion of life consumed per year

$$= \frac{1}{2\pi} \sum_{\text{sea states}} T(A) \sum_{\text{frequencies}} \frac{\omega}{\sigma^2} \int_0^{\infty} \frac{S \exp(-S^2/\sigma^2)}{N(S)} dS \dots (33)$$

hence the expected fatigue life has been obtained.

RESULTS AND CONCLUSIONS

The above analysis was performed on level 3 of the structure shown in Figure 1. The section analysed is shown in Figure 8. This level was chosen as it is the one nearest to the free surface and is hence in the region of greatest wave forcing. In order to look at this level in isolation the elements connecting to other levels were fixed at the far end to represent the presence of the rest of the structure. The lift forcing was applied in two ways.

- (i) Using a static analysis and assuming coherence of the lift forcing across the incident wave crest.
- (ii) Using the method of analysis outlined above which includes dynamic amplification effects and makes allowance for the random phase of the lift force between adjoining members.

Table 1 shows the results of this analysis for the section in Figure 8. The concentrated stresses are in the horizontal plane, and correspond to the seventh harmonic of the forcing wave with amplitude of 7.3 metres and of frequency .0557 Hz. The wave direction is North-South, which is along the lengthwise direction of the frame. The stresses at the four corner nodes are shown, together with the two mid-point nodes on the longer sides. The stresses obtained using the method described above are up to 27 times those obtained assuming coherent deterministic loadings throughout the frame. It is likely that dynamic magnification effects alone would account for this discrepancy between the two sets of calculated stresses, which indicates that they are due mainly to the differing phases between the forces on adjoining members.

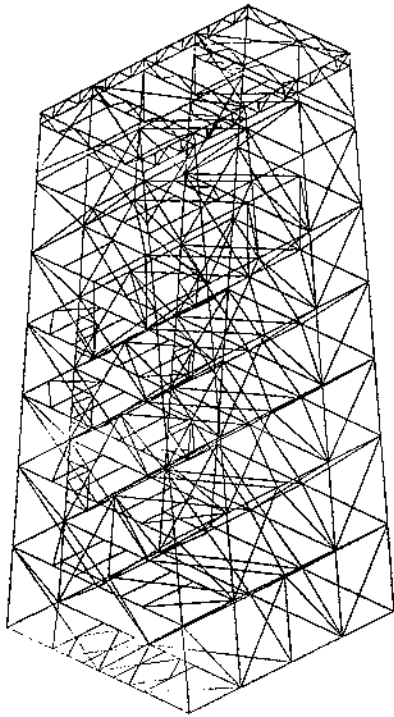
Hence the effects of vortex-shedding, as described by the above theory, should be taken into account in the assessment of the fatigue-life of off-shore structures.

REFERENCES

1. Johnson, R. Bretherton, I. and Tomkins, B: "The Effects of Sea Water Corrosion on Fatigue Crack Propagation in BS 4360: S0D Steel", Interim Technical Report UKOSRP 3/06, D.O.E. U.K. Offshore Steels Research Project, June 1979.
2. Miller, B.L.: "Wave Slamming Loads on Horizontal Circular Elements of Offshore Structures", NMI Report R22.
3. Holmes, P. Chaplin, and Flood, C.: "Wave Slamming Loads on Horizontal Members", Technology Reports Centre Report OT-R-7706, 1976.
4. University of Southampton Wolfson Unit: "An Investigation into Wave Slamming Loads on Cylinders", (OSFLAG 2A) Technology Reports Centre, OT-R-7743, 1977.
5. Brebbia, C.A. and Walker S.: "Dynamic Analysis of Offshore Structures", Newnes-Butterworths (Book) Dec 1979, 323 pp.
6. Kuang, A.B. Potvin, A.B. and Leide, R.D.: "Stress Concentration in Tubular Joints", OTC paper 2205, 1975.
7. Sarpkaya, T.: "In-Line and Transverse forces on Cylinders in Oscillatory flow at High Reynolds Numbers", OTC 2533, 1976.
8. Percy, H.H.: "Mechanics of Wave Induced Forces on Cylinders. Some Observations of Fundamental Features of Wave Induced Viscous Flows Past Cylinders", (Ed Shaw T.L.), Pitman 1979.
9. Morison, J.R. O'Brien, M.P. Johnson, J.W. and Schaaf, J.A.: "The Force Exerted By Surface Waves on Piles", Petrol Trans, AIME 189 1950.
10. Keulegan, G.H. and Carpenter, L.H.: "Forces on Cylinders and Plates in an Oscillating Fluid", Journal of Research of Natural Bureau Standards 60, No 5, pp 423-440 (1958).
11. Department of Energy, "Offshore Installations Guidance on Design and Construction", July 1977.

TABLE 1
CONCENTRATED STRESSES AT SELECTED
JOINTS N/M²

Stress Amplitudes Static Analysis	Standard Deviations Dynamic/Statistical Approach
2.6×10^5	7.0×10^6
6.2×10^5	1.6×10^6
4.5×10^5	8.6×10^6
3.8×10^5	7.8×10^6
2.9×10^5	6.7×10^6
6.5×10^5	1.7×10^6
4.9×10^5	1.3×10^6
3.8×10^5	1.1×10^6



JACKET STRUCTURE FIGURE 1

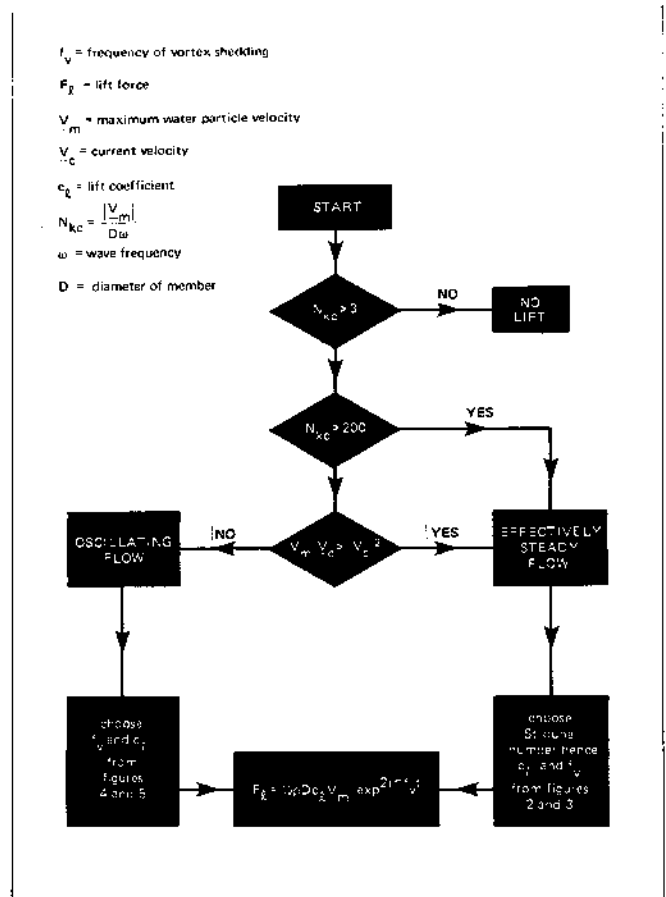
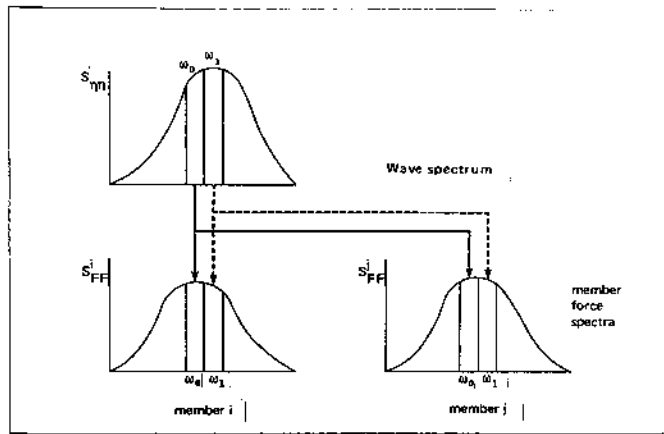
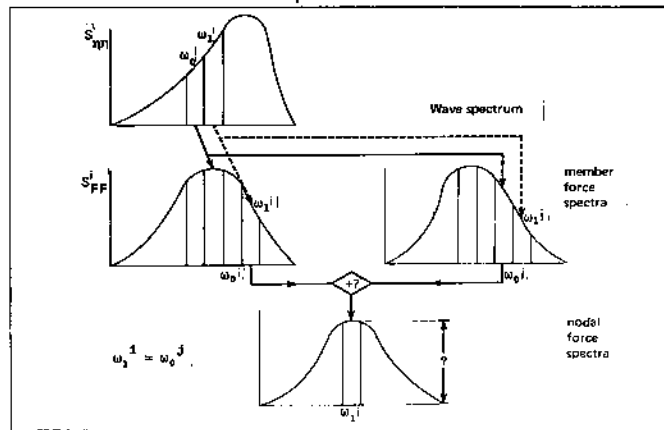


FIGURE 2



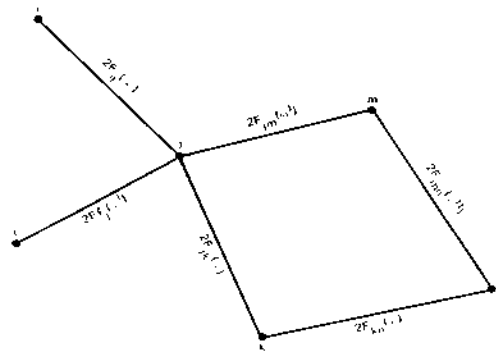
Direct Loading Drag and Inertia

FIGURE 3



Wave Loading Lift Forces

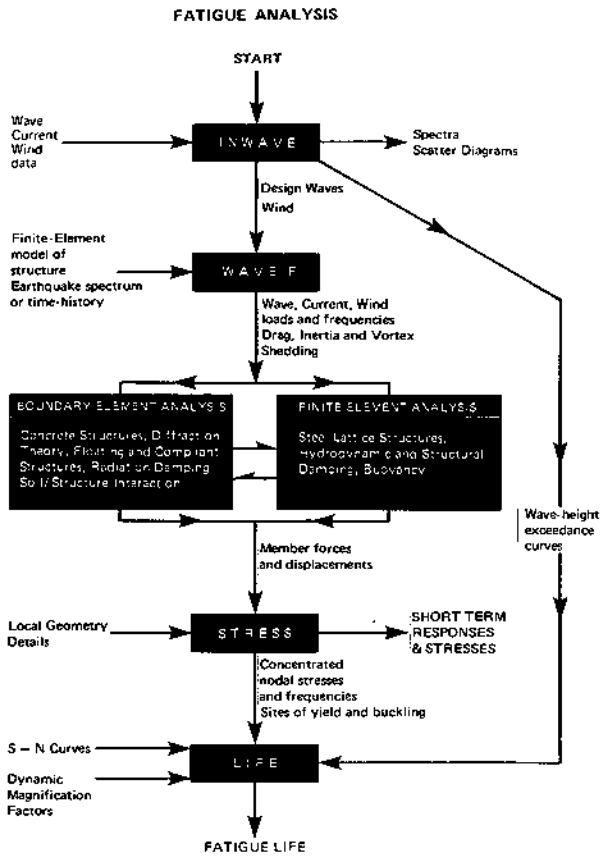
FIGURE 4



force on member $ij = 2F_{ij}(\omega)$ equivalent nodal force on node $i = F_i(\omega)$

$$F_k(\omega) = F_{jk}(\omega) + F_{kn}(\omega)$$

Part of the structure showing notation for member and nodal forces. FIGURE 5



System Overview

FIGURE 6

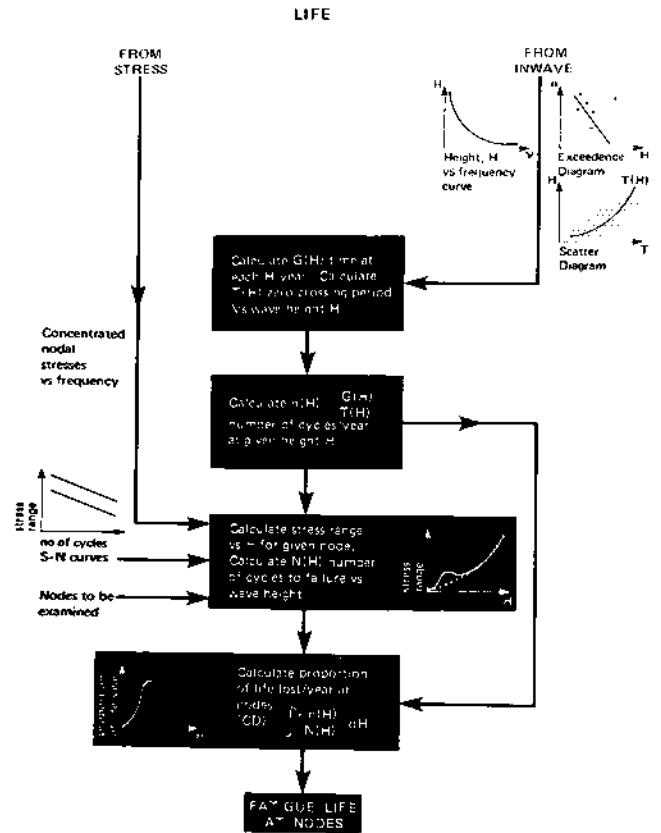
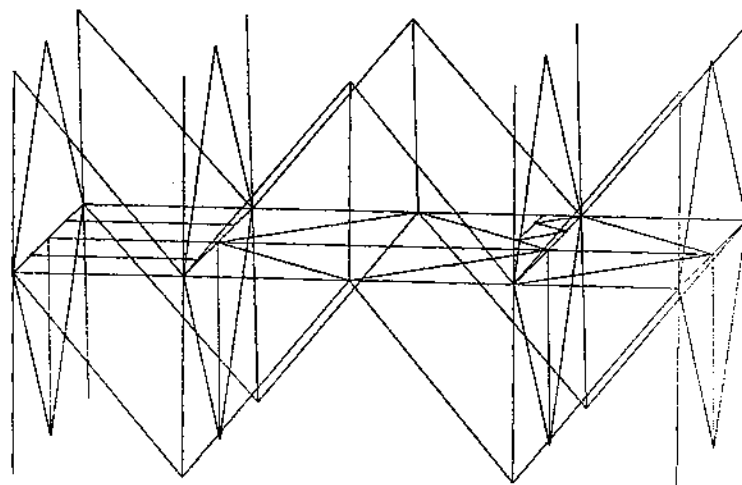


FIGURE 7



LEVEL 3 OF STRUCTURE

FIGURE 8

